

# COORDINATE EFFECTS ON THE USE OF ORBIT ERROR UNCERTAINTY

James Woodburn<sup>(1)</sup> and Sergei Tanygin<sup>(2)</sup>

<sup>(1)</sup> *Analytical Graphics, Inc., 220 Valley Creek Blvd., Exton, PA 19340, USA, +16109818082, [woodburn@agi.com](mailto:woodburn@agi.com)*

<sup>(2)</sup> *Analytical Graphics, Inc., 220 Valley Creek Blvd., Exton, PA 19340, USA, +16109818030, [stanygin@agi.com](mailto:stanygin@agi.com)*

**Abstract:** *Knowledge of spacecraft orbit uncertainty is becoming increasingly important for spacecraft operations and Space Situational Awareness. For cases where uncertainty is large, such as early orbit operations or anomaly situations, the manner in which orbit uncertainty is used and interpreted can be the difference between making correct or errant assessments of the effect of orbit uncertainty on spacecraft operations. The influence of coordinate selection on the proper utilization of orbit error covariance is examined and compared with the application of the unscented transform as a means to overcome issues of non-linearity. The use of preferential coordinates is seen to be of primary importance in the characterization of uncertainty while unscented transformations are seen to be effective at increasing the size of the uncertainty but are not able to overcome coordinate deficiencies to yield properly shaped uncertainty volumes.*

**Keywords:** *covariance, coordinates, linearity, orbit, uncertainty.*

## 1. Introduction

Knowledge of the uncertainty in the trajectories of spacecraft is becoming increasingly important for use in spacecraft operations and Space Situational Awareness (SSA). Applications include verification of orbit accuracy requirements, automated tracking data validation, determination of statistical consistency between orbit trajectories, association of observations with specific spacecraft and conjunction assessment. Historical practices involving the exchange of orbit trajectory information often included only the nominal orbit solution with no information about the accuracy of the solution. The exchange of two line element sets is one very common example of this type of trajectory exchange. Modern standards for the exchange of orbit trajectory information reflect the increasing importance of accuracy knowledge and facilitate the inclusion of trajectory uncertainty information in the form of orbit error covariance [1].

Actual error distributions associated with orbit estimates are described by an unknown probability density function. It is common practice, however, to assume that orbit errors have a zero mean and are Gaussian distributed. Under these assumptions, the set of all possible trajectories may be represented by a nominal orbit and an associated orbit error covariance matrix. When orbit errors are small as is typical for operational satellites under cooperative tracking, it is generally accepted that the assumption of a Gaussian error distribution is reasonable. Under conditions of larger orbit uncertainty, non-linear effects become important and the assumption that the errors are Gaussian distributed must be tested. While not typical in operations, such instances of large uncertainty can exist during early orbit operations and during anomaly situations. On the other hand, large orbit uncertainty is not at all uncommon in space surveillance where tracking data on small objects can be sparse and the need to generate an orbit from a small number of observations is common.

The goals of the following analyses are to demonstrate the effect of using different coordinates to represent uncertainty and to compare the covariance representations in those coordinates when computed via linear and non-linear transformations. Distributions will be represented as a mean and associated error covariance without the benefit of higher order moments. We assume that the estimate of the mean and the associated error covariance are produced by an orbit determination process. We further assume that the nominal trajectory and the associated error covariance have been provided via data exchange. The availability of a mean orbit trajectory and associated error covariance is consistent with the information content available from commonly used orbit estimation methods such as Batch Weighted Least Squares (BWLS) and the Extended Kalman Filter (EKF) [2]. More recently developed estimation strategies such as the Unscented Kalman Filter (UKF) [3] and its variants which have grown in popularity are also based on knowledge of a mean orbit and associated error covariance. Other orbit determination strategies which are designed to handle cases where the orbit error distribution cannot be adequately modeled as being Gaussian, such as the use of the summed Gaussian distributions [4], are not considered since the additional information required to represent the orbit error uncertainty is not available in current trajectory exchange formats.

The nominal trajectory and associated error covariance are typically provided in a single set of coordinates. Conversion of the trajectory to additional sets of coordinates is achieved through non-linear transformations. We assume that these non-linear transformations are exact and invertible such that the trajectory representation is equivalent in all coordinates. Conversion of covariance information between different sets of coordinates can be achieved in a linear transformation using the Jacobian [5] between the two sets of coordinates or through a non-linear technique such as the unscented transform [3]. Coordinate independence, such as that of the trajectory representation, does not generally exist for the covariance. The extent to which the covariance accurately represents the actual orbit error probability density function will strongly influence the validity of subsequent computations which require that covariance as an input. When orbit uncertainties are small as in normal operations, any set of coordinates can typically be used with equal validity and the problem is considered to be linear. As the orbit uncertainty increases, judicious coordinate selection can sometimes greatly expand the valid domain for the assumption of a Gaussian error distribution. For example, the comparison of trajectory differences to the orbit error covariance using orbital elements produces much more satisfactory results compared to performing the comparisons in Cartesian coordinates [6-8].

Given that preferential coordinates exist for the representation of orbit uncertainty, we would always choose to work in these coordinates if possible. Unfortunately, particular computations which use orbit uncertainty information may require that the orbit uncertainty be expressed in coordinates which are natural for those applications. For example, the use of covariance information to provide probability based gating for observation acceptance during sequential orbit determination typically requires the orbit error covariance to be transformed into measurement space to enable the required accept/reject decision. The likelihood of making the correct accept/decision will depend on how well the covariance transformed to measurement space represents the actual orbit error distribution.

In this study, we examine coordinate effects on two common operational uses of orbit uncertainty information: trajectory comparisons and tracking data validation. Our analyses will include numerical and visual results which will promote intuitive understanding of the effects of coordinate selection on the studied problem set. In cases where the natural coordinate selection leads to poor representation of the orbit uncertainty, we will explore alternate formulations in an attempt to minimize the effects of non-linearity. While other studies have provided means for numerical evaluation of covariance realism [9-12], the analyses presented here are primarily qualitative in nature with the intent of identifying recommended practices as opposed to providing specific metrics by which uncertainty realism can be measured.

## 2. Analyses

Under the assumption that the probability density function associated with an orbit error distribution is Gaussian, all possibilities for the true trajectory are represented by an orbit estimate and its associated orbit error covariance. As mentioned above and as we will demonstrate below, the validity of the Gaussian assumption is greatly dependent upon the coordinates in which the errors are represented. Since a user of orbit uncertainty information will typically have little influence on how that information is derived or delivered, the goal must be to utilize best practices in how the data is used.

Different sets of coordinates are related via non-linear transformations. In the following analyses, transformations of covariance information will be performed linearly and through the Unscented Transform (UT). Let  $X$  represent the orbit state as expressed in Cartesian coordinates and  $\alpha$  represent the orbit state as expressed in another set of coordinates (such as orbital elements). The non-linear transformations between the two sets of coordinates are given as

$$X = G(\alpha) \quad (1)$$

and

$$\alpha = U(X). \quad (2)$$

Small deviations from the nominal trajectory are linearly mapped between the different sets of coordinates using the Jacobian matrices

$$\Delta X = \frac{\partial X}{\partial \alpha} \Delta \alpha + \text{H.O.T.} \quad (3)$$

and

$$\Delta \alpha = \frac{\partial \alpha}{\partial X} \Delta X + \text{H.O.T.}, \quad (4)$$

where H.O.T. represents higher order terms. The linear transformation of the covariance is achieved through the use of the same Jacobian matrices,

$$P_X = \frac{\partial X}{\partial \alpha} P_\alpha \frac{\partial X^T}{\partial \alpha} \quad (5)$$

and

$$P_\alpha = \frac{\partial \alpha}{\partial X} P_X \frac{\partial X^T}{\partial \alpha} . \quad (6)$$

The linear transformations have the desirable properties of being independent of the sequence of coordinates used during the transformation process and being invertible, outside of coordinate induced singularities.

Using the unscented transform, one converts a set of judiciously selected samples from the original error distribution to the new coordinates using the non-linear coordinate transformation and computes the mean and covariance in the new coordinates from the weighted samples [3]. As there are multiple ways to select the weights and associated sample (sigma) points, the reader is referred to Julier [3, 13-15] for details on particular point selection algorithms. Let  $X_k$  represent a set of M Cartesian sigma points (typically  $2N+1$  points where N is the dimension of the estimation state) and  $W_k$  represent the weights associated with those points. Then the unscented transformation from Cartesian to other coordinates alpha is represented as

$$\alpha = \sum_k W_k U(X_k), \quad (7)$$

$$P_\alpha = \sum_k W_k [(U(X_k) - \alpha)(U(X_k) - \alpha)^T]. \quad (8)$$

The inverse transformation, from another set of coordinates to Cartesian coordinate is described as

$$X = \sum_k W_k G(\alpha_k), \quad (9)$$

$$P_X = \sum_k W_k [(G(\alpha_k) - X)(G(\alpha_k) - X)^T]. \quad (10)$$

We start our examination by looking at trajectory comparisons and leverage those results in the determination of measurement validity. In each case, multiple levels of orbit uncertainty will be examined to allow the reader to evaluate results in a context appropriate to his/her needs. We will show that selection of proper coordinates is of primary importance when orbit errors become large.

## 2.1. Orbit Uncertainty

Orbit uncertainty information is commonly used in trajectory comparisons to determine if operational orbit accuracy requirements are satisfied and to evaluate consistency between multiple orbit solutions. It has been well documented that specifying the uncertainty of an orbit in Cartesian coordinates does not provide a satisfactory representation as the uncertainty in the orbit grows [6-8]. It has also been shown that orbit uncertainty specified in Cartesian coordinates can be linearly transformed to orbital elements to provide a much more satisfactory result. The advantage gained in orbital elements is primarily due to the ability to capture the dominant part of the uncertainty growth without approximation [5]. Based on improved estimation performance and an improved representation of the orbit error uncertainty, one can make a strong case for the use of orbit elements to express orbit trajectories and uncertainty.

Most orbit accuracy requirements and downstream analyses, however, are not simply expressed in terms of orbital elements and therefore do not allow for direct use of orbit uncertainty expressed in this manner. Of particular interest is the ability to express orbit position uncertainty in terms of distances. We therefore desire to choose coordinates which are able to represent the uncertainty in position and velocity separately in addition to having a connection to the dynamics of the orbit trajectory.

Curvilinear coordinates have been developed for improved uncertainty modeling and have the desirable feature, as compared with orbit elements, that position and velocity uncertainty are readily examined independently. Vallado defines a set of curvilinear coordinates based on modified Equidistant Cylindrical coordinates which are well suited for use in proximity operations and uncertainty representation [16]. The transformation from Earth Centered Inertial (ECI) coordinates and the modified Equidistant Cylindrical coordinates is goes through the radial/transverse/cross-track frame (referred to as RSW coordinates) and requires the solution on an elliptic integral. Hill defined a set of curvilinear coordinates based on normal/tangential/cross-track reference frame (referred to as cNTW coordinates) where the cN and cT coordinates follow the contour of the osculating orbit ellipse as you move away from the location of the spacecraft [7]. It was further approximated that covariance information mapped to NTW coordinates could simply be reinterpreted as being relative to cNTW coordinates. This mapping/interpretation of the covariance was seen to provide a much better representation of the actual orbit error distribution than Cartesian coordinates. Figure 1 is a reproduction of Fig. 2 from Hill and shows how the cNTW coordinate directions are defined relative to the instantaneous osculating ellipse associated with the nominal orbit trajectory [7]. For reasons of simplicity, we have chosen to use the curvilinear coordinates as defined by Hill in this analysis.

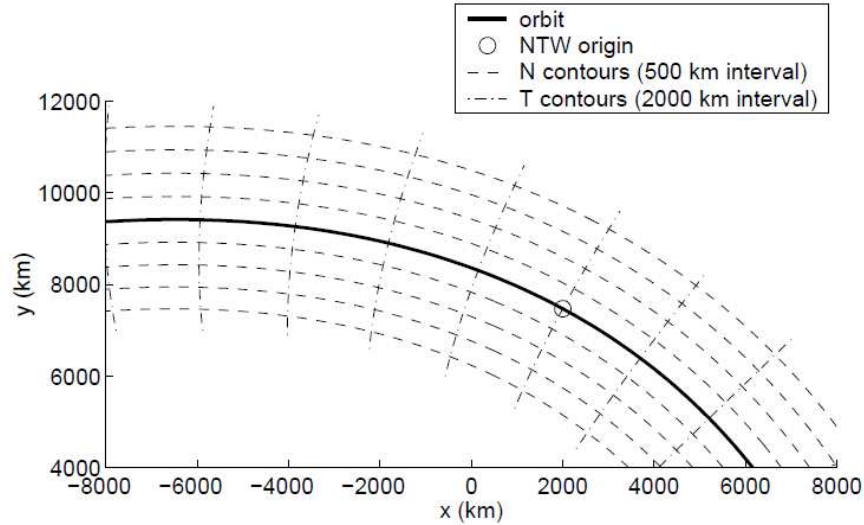


**Figure 1. Hill Figure 2: cNTW Coordinates**

Table 1 provides the orbital elements for a Low Earth Orbit (LEO) test case. The approximate initial uncertainties were extracted from a full orbit error covariance generated by processing simulated tracking data over a period prior to the start of the test. Tests at different levels of orbit uncertainty, as shown in Table 2, are facilitated by propagating the orbit and the full orbit error covariance into the future until the desired levels of tangential uncertainty were achieved. The values given for uncertainty in the normal and cross-track directions represent approximate averages of the oscillating values over one revolution at the prediction time for each test case.

**Table 1. Approximate Orbital Elements for LEO Test Case**

Semi-major axis	7000 Km
Eccentricity	0.005
Inclination	98.7 Deg
Right Ascension of Ascending Node	0.0 Deg
Argument of Perigee	90.0 Deg
Mean Anomaly	30.0 Deg

**Table 2. Approximate 1 Sigma Position Uncertainties**

Axis	Init. Cond.	Case I	Case II	Case III	Case IV
Normal	0.004 Km	0.010 Km	0.023 Km	0.043 Km	0.064 Km
Tangential	0.056 Km	1 Km	10 Km	100 Km	300 Km
Cross-track	0.003 Km	0.003 Km	0.004 Km	0.020 Km	0.044 Km
Prop Time	0	1 day	5.5 days	27 days	58.5 days

The main driver in the growth of the orbit uncertainty during prediction was the uncertainty in the ballistic coefficient (nominal value of 0.044 with a 50% short term uncertainty). The orbit position uncertainty expressed in normal, along-track and cross-track components during the fit

span are shown in Fig. 2, while Figs. 3-5 show the orbit uncertainty during the prediction period. During the prediction period, the tangential uncertainty grows in a secular fashion while uncertainty in the normal and cross-track directions grow more slowly with a strong oscillatory component. Due to how the end of the fit interval was placed, approximately 3 hours of prediction occurs between the end of the tracking data and the end of the fit interval where the initial condition values are measured for the prediction. The fact that the initial covariance was generated by processing simulated measurements in an orbit determination program is extremely important when the growth rate of the uncertainty is considered. A much larger, but not realistic in an operational scenario, growth rate is achieved when starting with an ad-hoc covariance which does not contain proper correlations to manage the energy uncertainty of the orbit estimate. A small Monte-Carlo sample set of 250 draws was constructed based on the 7x7 covariance (position, velocity and ballistic coefficient) at the end of the fit span. See Fig. 6 for a depiction of the initial sampling in relation to the 95% probability (2.795 sigma) position error covariance generated using Systems Tool Kit<sup>®</sup> [17] by AGI.

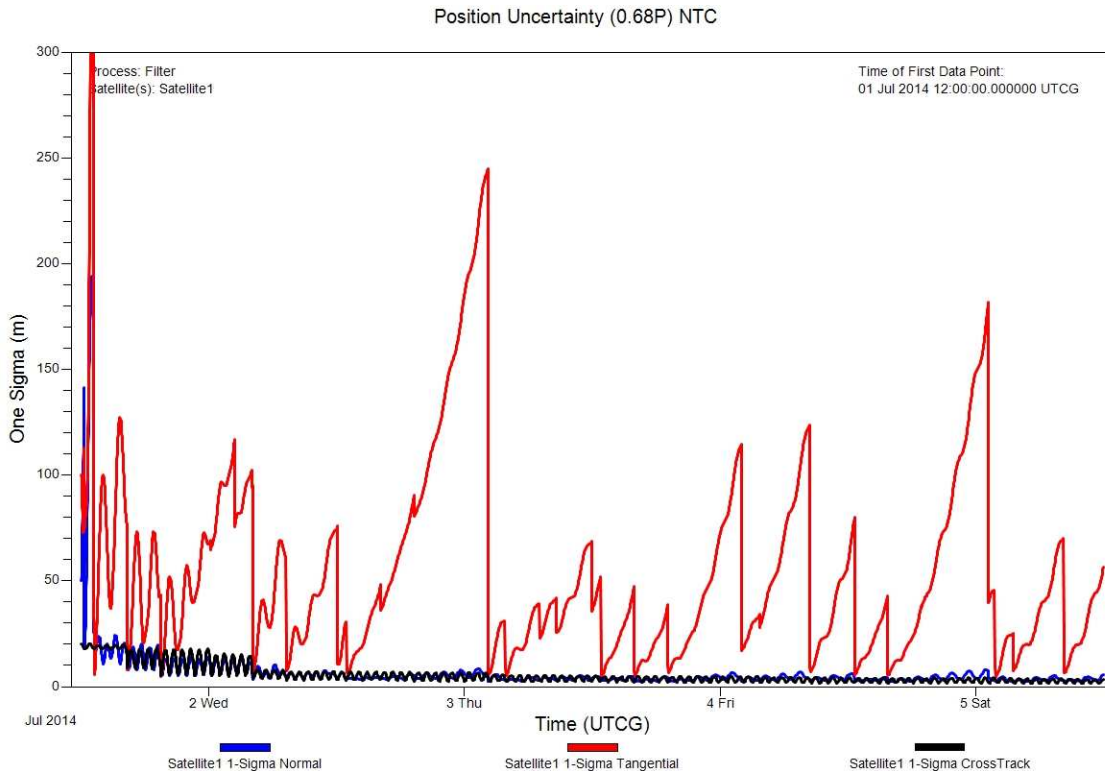


**Figure 2. 1 Sigma Orbit Position Uncertainty During Fit Span**

Position Uncertainty (0.68P) NTC

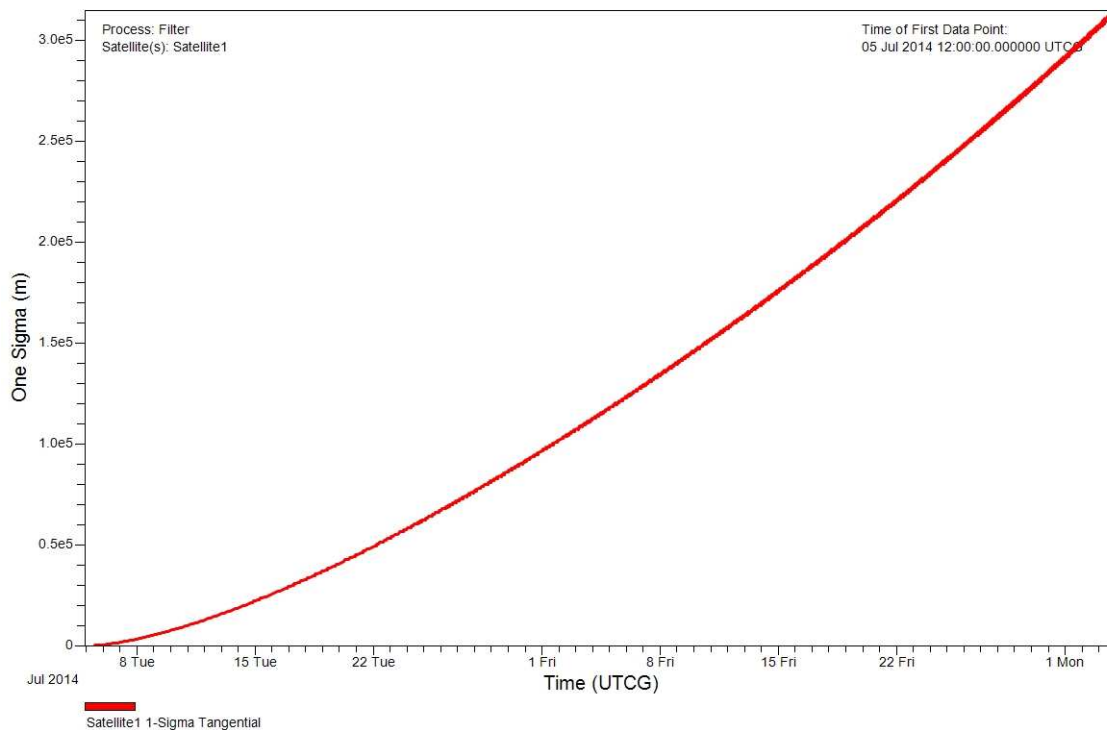


**Figure 3. 1 Sigma Tangential Position Uncertainty Prediction**

Position Uncertainty (0.68P) NTC

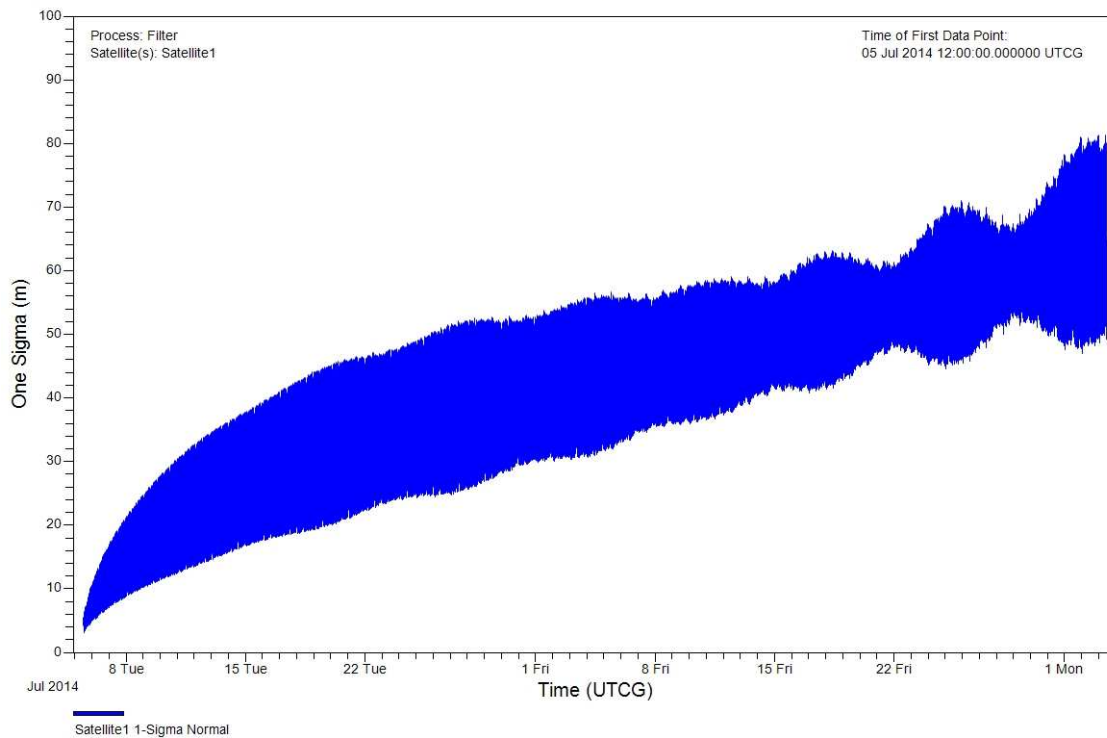


**Figure 4. 1 Sigma Normal Position Uncertainty Prediction**



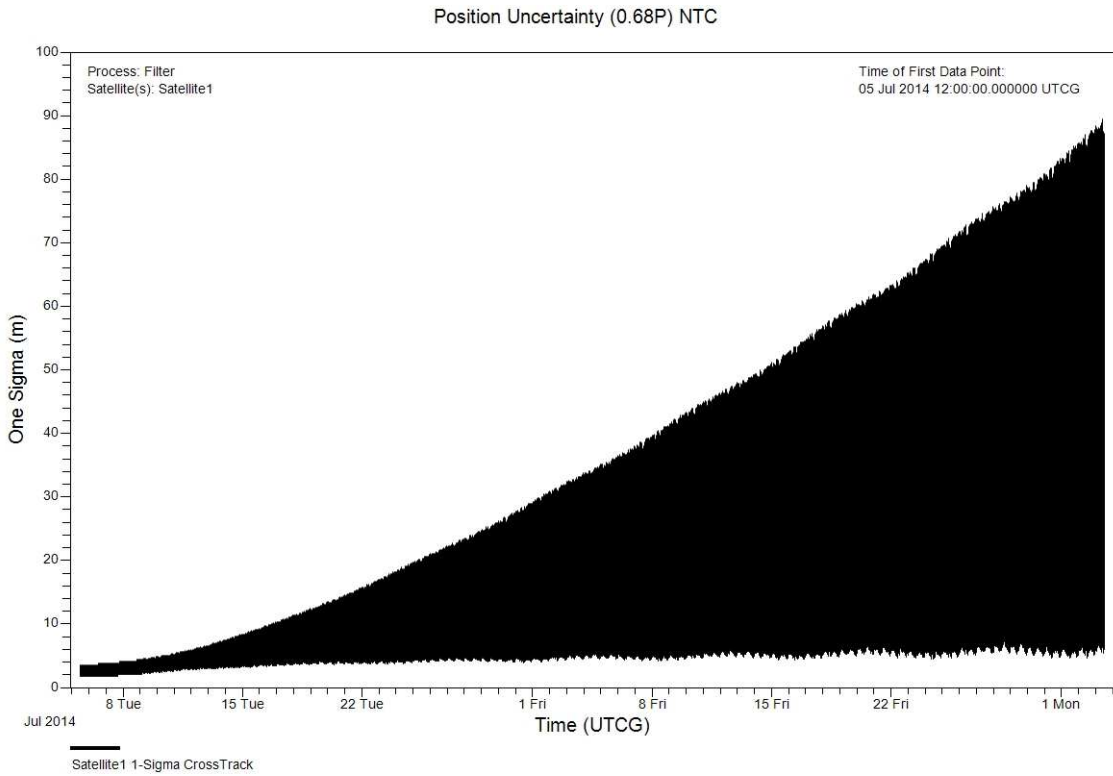


**Figure 5. 1 Sigma Cross-track Position Uncertainty Prediction**

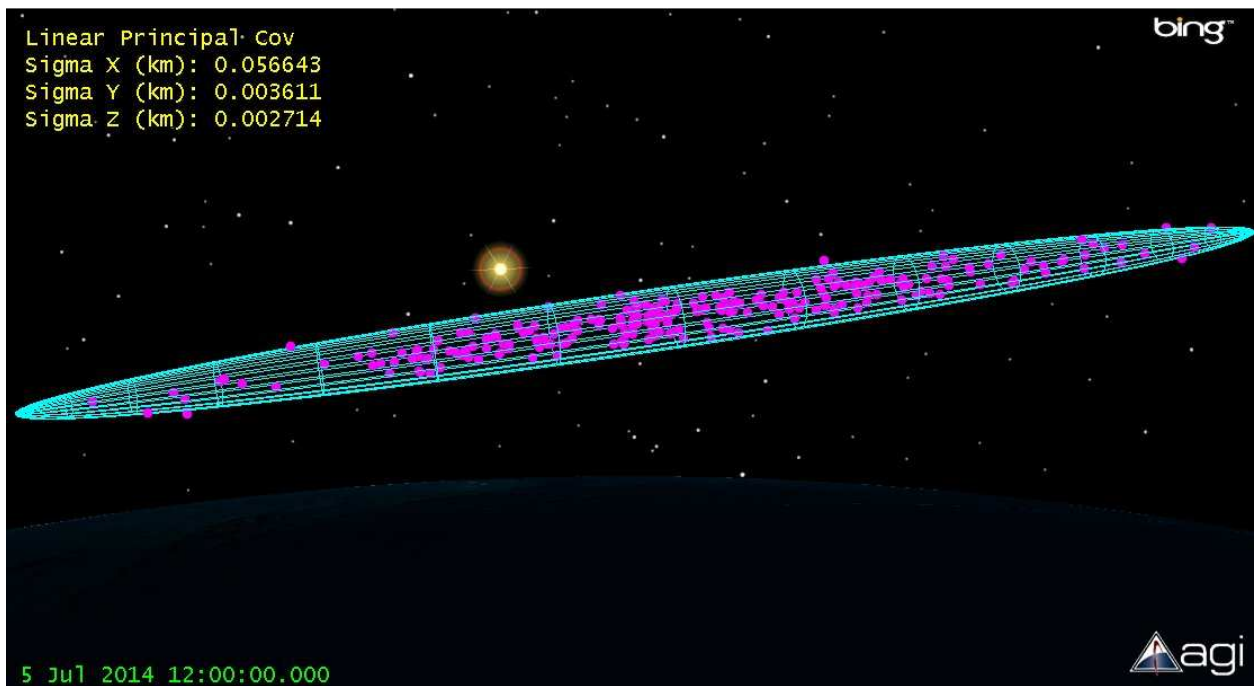


**Figure 6. 95% Monte-Carlo Initial Draws with 95% Probability Orbit Position Covariance Ellipsoid**

The initial covariance was generated and propagated forward in time using the EKF in the Orbit Determination Tool Kit<sup>®</sup> (ODTK), a commercial off the shelf orbit determination capability produced by AGI [18]. Starting with the ODTK output of orbit error covariance in Cartesian coordinates, we linearly transform the covariance from test cases I-IV to cNTW coordinates and visually inspect the level of agreement with the Monte-Carlo samples. After verifying that the representation in the linearly derived cNTW coordinates properly captures the Monte-Carlo samples, we use the covariance in cNTW coordinates as the input to the unscented transform to compute a new mean and covariance in Cartesian coordinates. We are then able to visually compare the three covariance representations (linear Cartesian, curvilinear, UT Cartesian) to the Monte-Carlo sample distribution.

The simultaneous graphical depiction of the various position covariance representations allows us to draw attention to the difference between coordinates which have preferred properties in terms of the representation of orbit error uncertainty and the use of higher order techniques, such as the unscented transform. Figures 7-10 show the results for Cases I-IV. The cyan colored ellipsoids are the orbit error covariance represented in cNTW coordinates, the yellow ellipsoids are the orbit error covariance in Cartesian coordinates and the green ellipsoids are the orbit error covariance mapped from cNTW coordinates into Cartesian coordinates using the unscented transform. In Fig. 7, which illustrates 1 Km (1 sigma) of tangential uncertainty, the difference between the covariance ellipsoids is essentially indiscernible. At a tangential uncertainty of 10 Km (1 sigma) as shown in Fig. 8, the position covariance ellipsoids are extremely similar with the unscented transform having the effect of expanding the uncertainty in the normal direction by a small amount.

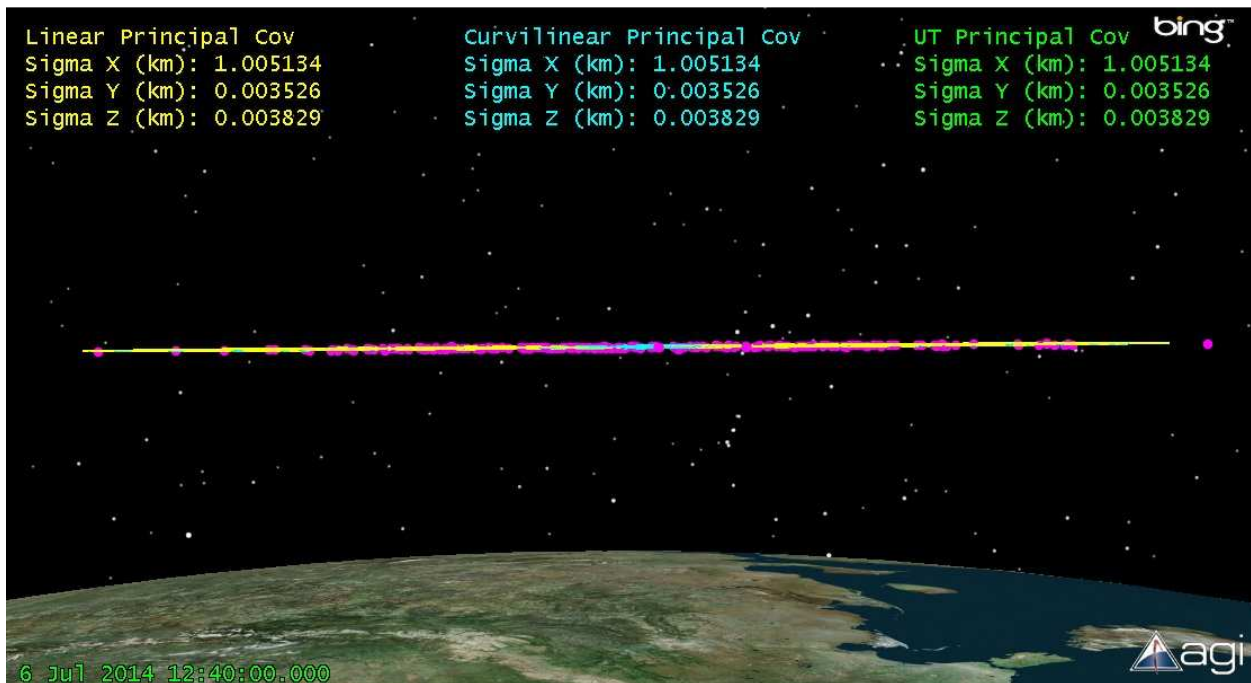
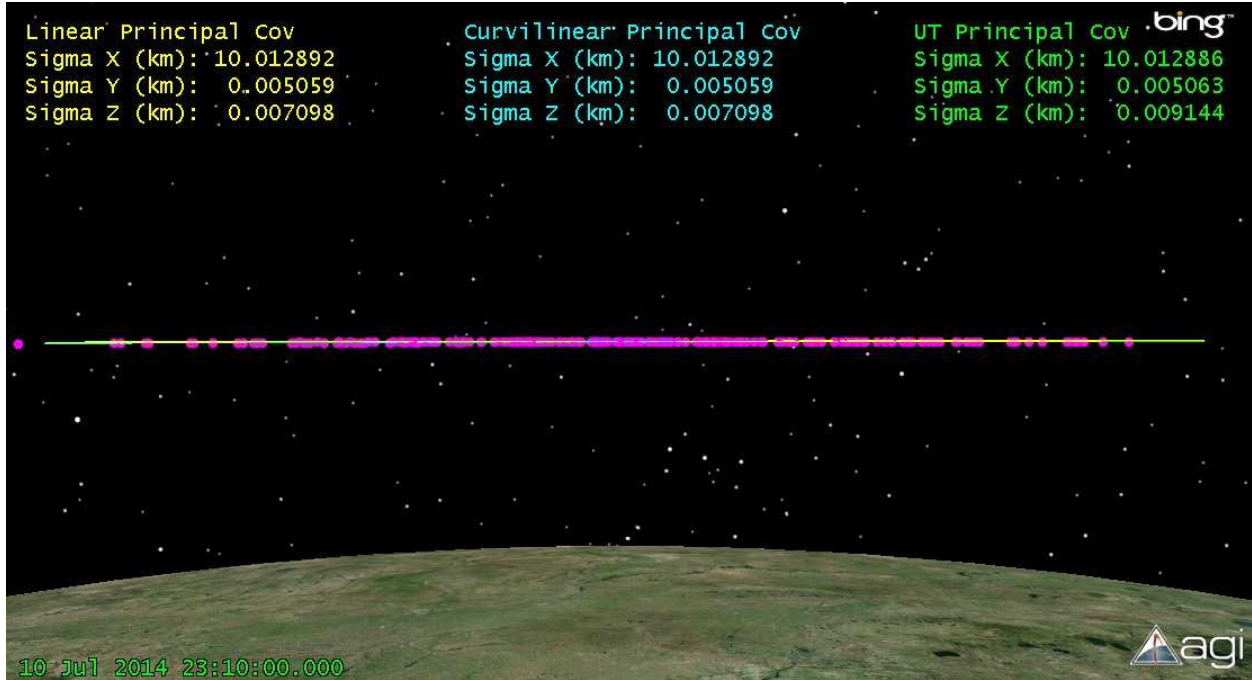
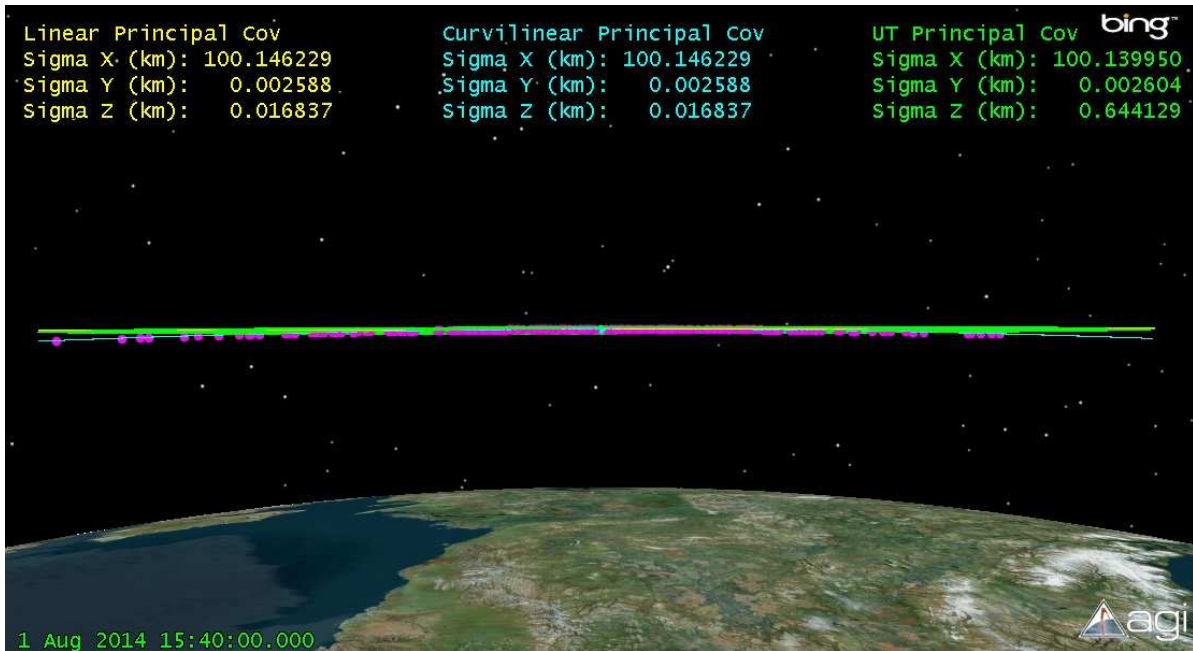


Figure 7. Case I: Orbit Position Uncertainty



**Figure 8. Case II: Orbit Position Uncertainty**

Figures 9-10 clearly demonstrate the preferential nature of the cNTW coordinates for the expression of orbit uncertainty for cases with large uncertainty. We note that the use of the unscented transform does not provide improvement in our ability to model the bending of the actual error distribution. Instead the covariance is simply enlarged in the normal direction which allows for more of the Monte-Carlo sample points to fall within the position error covariance ellipsoid. At this scale of error, the selection of coordinates in which the error is represented is much more important than the incorporation of higher order terms provided by the unscented transform. It is also worthy of mention that the mean of the distribution after the unscented transform is moved to a location off of the nominal orbit trajectory to a location of almost negligible likelihood based on the distribution in cNTW coordinates, see Figure 11.



**Figure 9. Case III: Orbit Position Uncertainty**

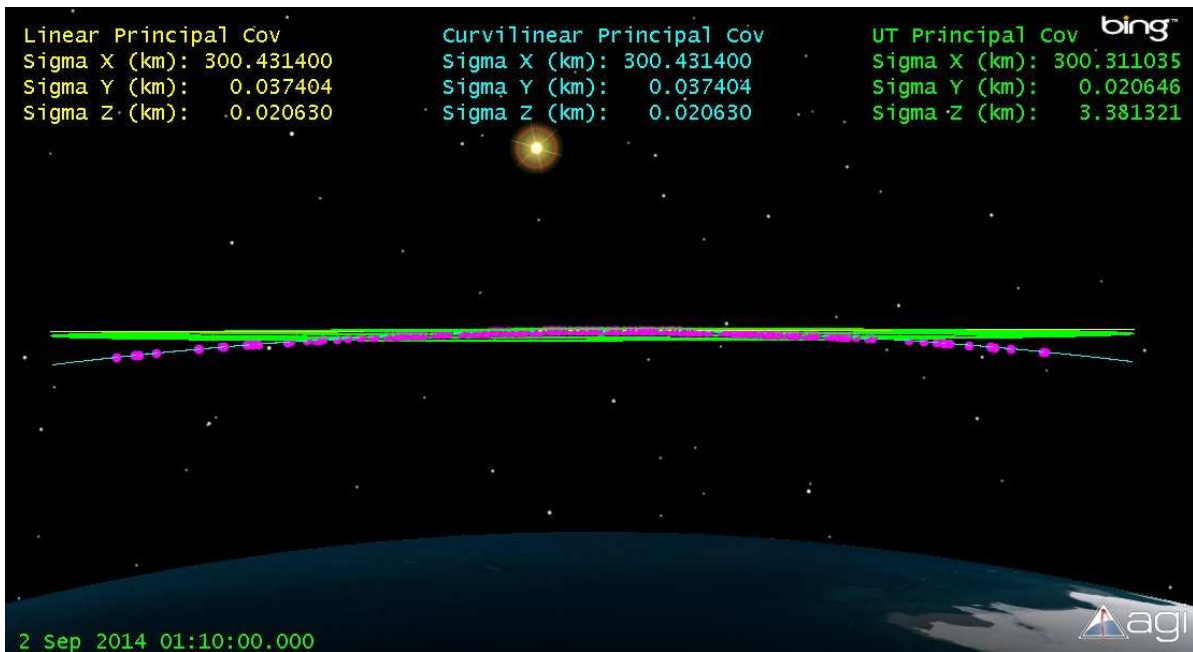


**Figure 10. Case I: Orbit Position Uncertainty**

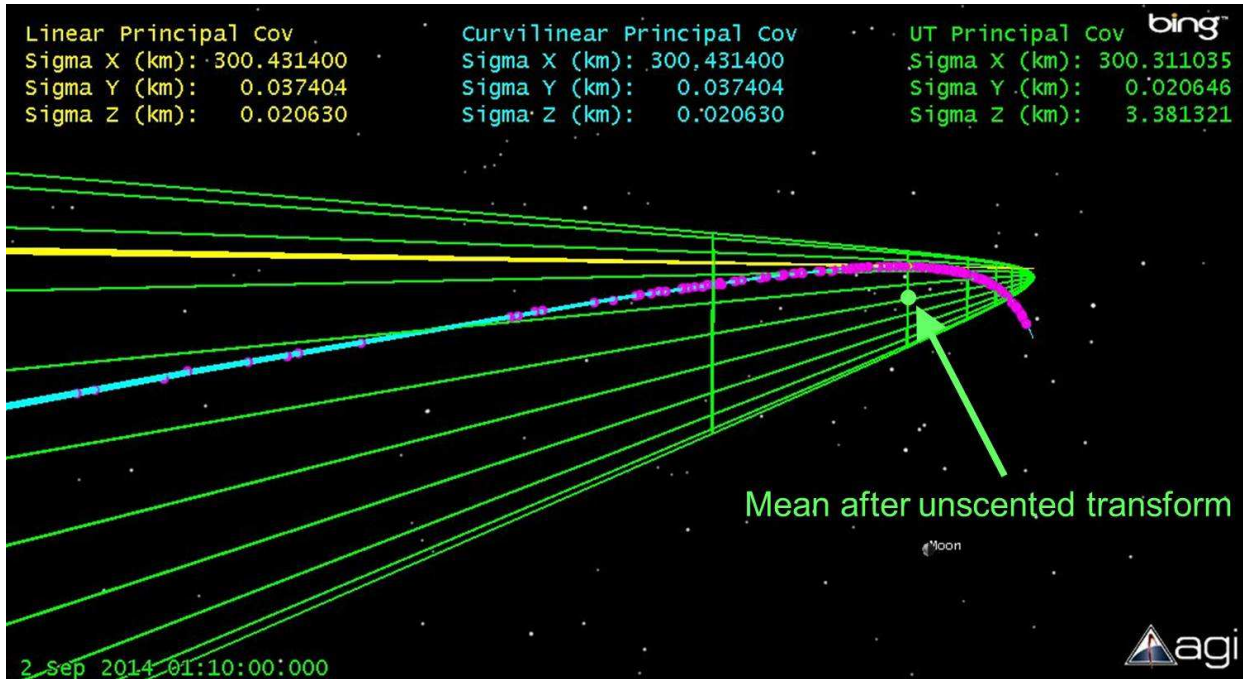


**Figure 11. Case IV: Offset of Mean from Unscented Transform**

Techniques for matching probability density functions such as Gaussian mixtures are sometimes used to provide a better model of the shape of the actual error distribution [19-20]. In this technique, a sum of weighted Gaussian probability density functions would be used in an attempt to model a non-Gaussian error distribution in Cartesian coordinates. While this methodology is certainly adaptable to the problem at hand due to the fact that any number of Gaussian components can be used, it is often the case for realistic orbit estimation scenarios that the additional complexity of the Gaussian sum can be avoided through the use of preferred coordinates.

## 2.2. Measurements

The ability to use orbit error uncertainty to determine the validity of measurements is important for automated data editing during orbit estimation and for the proper association of non-transponder based measurements, such as optical right ascension and declination or RADAR observations, when dealing with closely spaced spacecraft. When orbit uncertainty is small, the orbit covariance can be mapped directly to the space defined by the native measurements without significantly affecting the shape of the error distribution. When orbit errors become large, however, we are interested to determine if a conversion of measurements to different coordinates might provide improved outcomes in determining measurement validity.

To illustrate the effects of growing orbit uncertainty on the validity of covariance in measurement space, we leverage the test cases provided in Table 1. The orbit uncertainty is mapped into measurement space for an observation vector consisting of ground based azimuth, elevation and range (AER). Similar to our analysis of orbit uncertainty above, the mapping of the covariance will be performed both linearly and through the unscented transform. The linear

mapping will use the linearly generated result of the EKF in Cartesian coordinates as the input while the unscented transform will start with the covariance that has been linearly mapped to cNTW coordinates. We note that the linear mapping will produce the same final result in AER coordinates, regardless of the selection of intermediary coordinates. The result of the unscented transform, however, will be dependent upon the selection of intermediary coordinates. We choose to start the unscented transform in cNTW coordinates to ensure that the starting point of the transformation provides an accurate representation of the uncertainty. The AER measurement space has been selected since it is representative of common cooperative and space surveillance tracking while provides a measurement set that can be readily transformed to other coordinates.

For the purpose of this analysis, ground station locations were selected to yield an elevation angle in the vicinity of 40 degrees for each test case. The reader is reminded that the conditions for each case were selected from an orbit prediction based on when particular levels of tangential uncertainty were achieved. After the covariance was transformed to AER coordinates, it was then visualized in position space in STK for qualitative comparison to the orbit uncertainty in cNTW coordinates. Results for all test cases are shown in Figs. 12-15 where the cyan colored ellipsoids are the orbit error covariance represented in cNTW coordinates, the yellow ellipsoids are the orbit error covariance mapped linearly into AER coordinates and the green ellipsoids are the orbit error covariance mapped from cNTW coordinates into AER coordinates using the unscented transform. In Fig. 12, we see that at a one sigma uncertainty of approximately one kilometer, all of the error representations appear to be effectively equivalent.

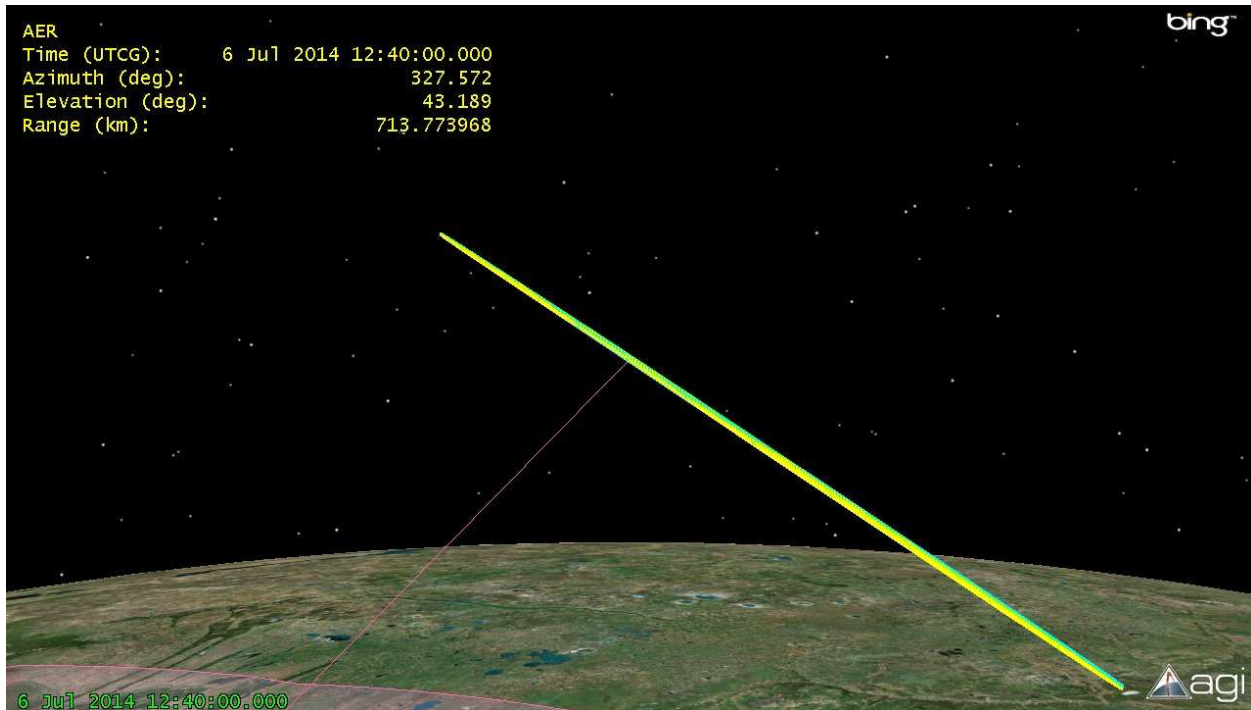


**Figure 12. Case I: Orbit Uncertainty Mapped to AER Coordinates**

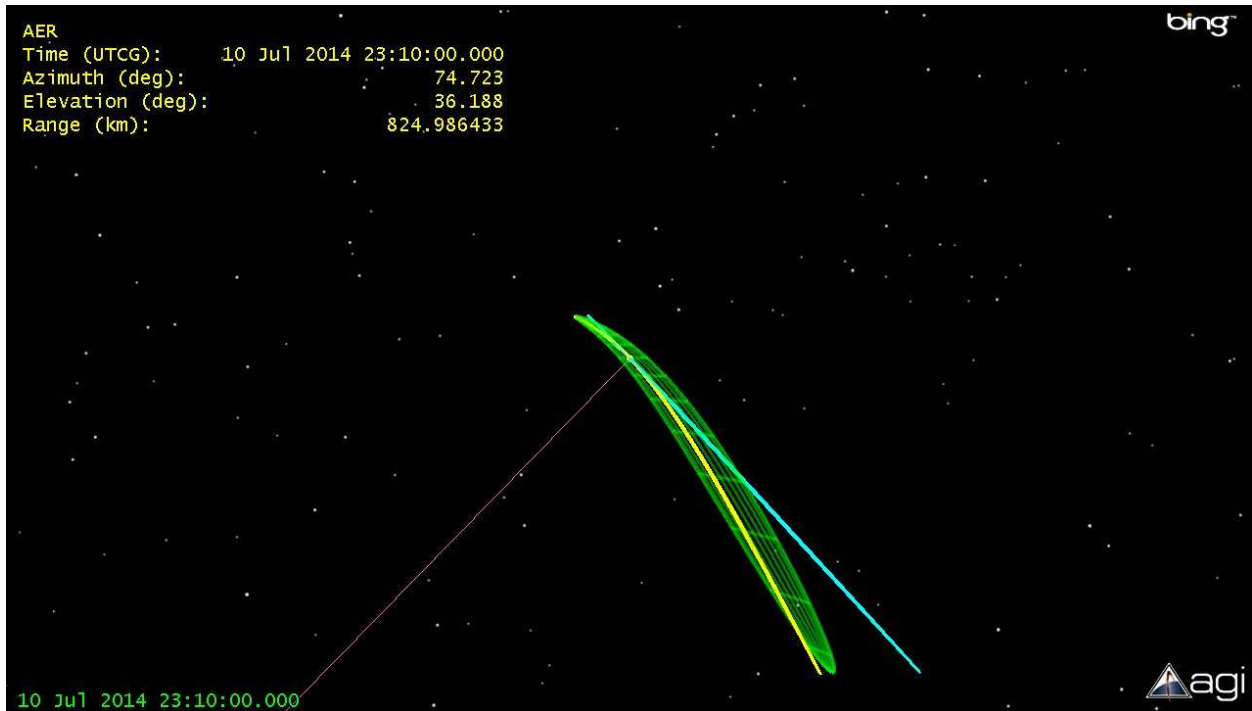


**Figure 13. Case II: Orbit Uncertainty Mapped to AER Coordinates**

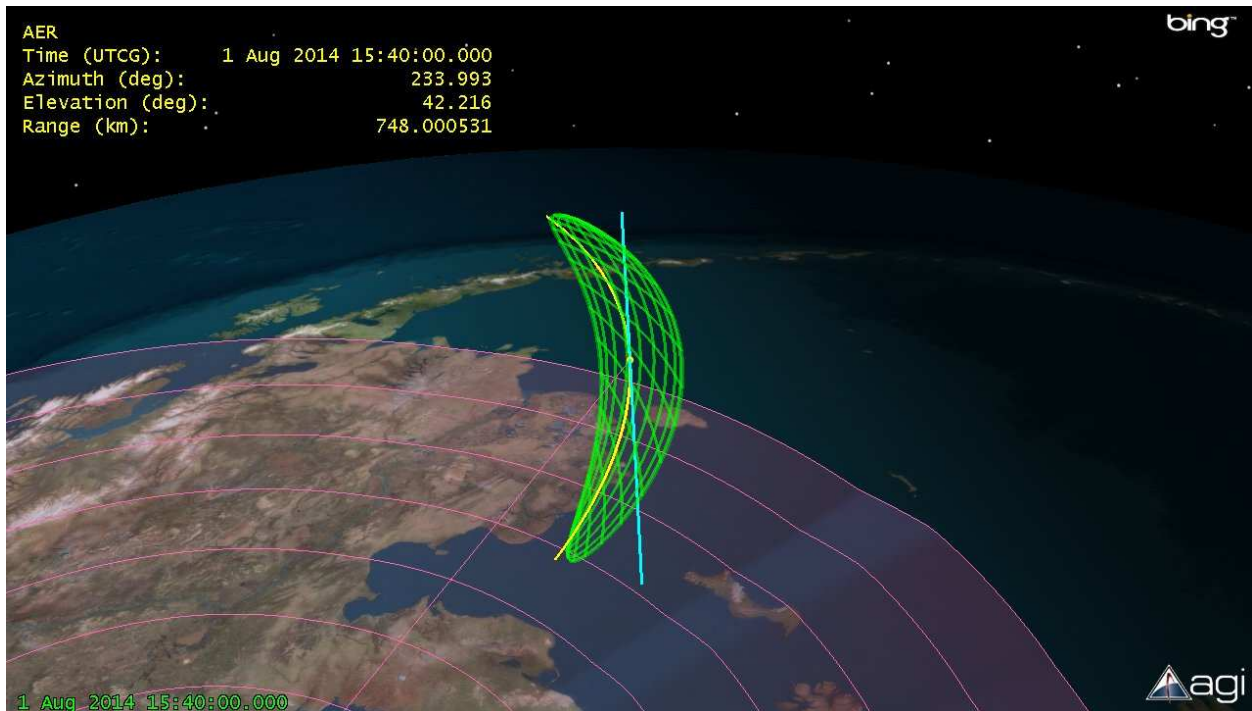


**Figure 14. Case III: Orbit Uncertainty Mapped to AER Coordinates**

Figure 13 shows that, at 10 kilometers of tangential uncertainty, the error volumes generated in AER coordinates are beginning to bend away from the cNTW representation which we trust to be accurate. By the time the tangential uncertainty reaches 100 kilometers, see Fig. 14, the bend

in the AER coordinate representation of the orbit uncertainty is very apparent and could easily lead to incorrect evaluations of the validity of observation sets. Finally, Fig. 15 shows the severe distortion that occurs at a tangential uncertainty of 300 kilometers. In the cases with larger tangential uncertainty, the unscented transform results in a covariance which encompasses a larger percentage of the cNTW uncertainty volume which indicates a small chance of flagging good measurements as invalid. On the other hand, the UT generated covariance also encompasses a great deal of space where measurement rejection would be appropriate thus leading to an increased chance of accepting poor measurements. It is important to note that the level of distortion seen in these graphics is directly related to the ratio of the range between the ground station and the satellite. Similar levels of uncertainty would produce smaller amounts of bending in the AER coordinate representation of the uncertainty for satellites at higher altitudes.

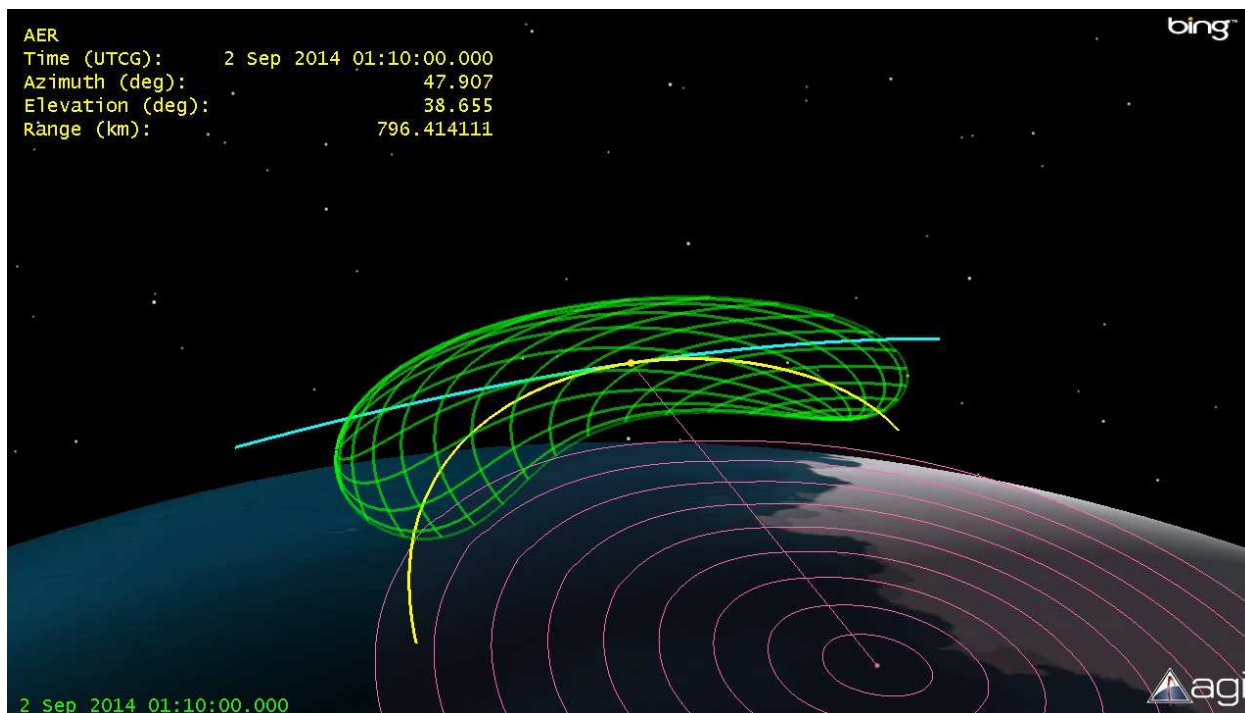


**Figure 15. Case I: Orbit Uncertainty Mapped to AER Coordinates**

The good news, in the case of AER measurements, is that this problem can be avoided to a large degree by performing a non-linear transformation of the AER measurement set into a Cartesian position. The resulting Cartesian position can then be evaluated against the orbit error covariance in cNTW coordinates, similar to how the Monte-Carlo samples were compared, to take advantage of the linear properties of these coordinates.

### 3. Conclusions

Coordinate selection is of primary importance in the representation of large orbit uncertainty. Coordinates which naturally conform to the shape of the trajectory such as the cNTW coordinates and orbital elements may be used in a very simple manner to provide covariance representations which adequately model the orbit error distribution to levels of at least several



hundred kilometers in LEO. The unscented transform has the effect of expanding the covariance to better encompass the range of samples generated from the Monte-Carlo analysis, but does not facilitate bending of the covariance in Cartesian or AER coordinates to provide improved conformity to the shape of the error distribution. Large orbit uncertainty can exhibit significant non-linear effects when mapped into measurement space. In some cases, it may be possible to perform a non-linear transformation on the measurements so that evaluations of measurement validity can be performed in preferred coordinates.

#### 4. References

- [1] Orbit Data Messages. Recommendation for Space Data System Standards, CCSDS 502.0-B-2. Blue Book. Issue 1. Washington, D.C.: CCSDS, November 2009.
- [2] Tapley, B.D., Schutz, B.E., Born, G.H., Statistical Orbit Determination, Elsevier, 2004.
- [3] Julier, S.J., Uhlmann, J. K., and Durrant-Whyte, “A new approach for filtering nonlinear systems,” 1995 American Control Conference, Seattle, WA, pp. 1628–1632.
- [4] DeMars, K. J., and Jah, M.K., "Probabilistic Initial Orbit Determination Using Gaussian Mixture Models", Journal of Guidance, Control, and Dynamics, Vol. 36, No. 5 (2013), pp. 1324-1335.
- [5] Woodburn J., Coppola, V., “Effect of Coordinate Selection on Orbit Determination”, AAS 13-825, 2013 AAS/AIAA Astrodynamics Specialists Conference, Hilton Head, SC, August 2013.
- [6] Junkins, J. L., Akella, M. R., and Alfriend, K. T., “Non-Gaussian Error Propagation in Orbit Mechanics,” Journal of the Astronautical Sciences, Vol. 44, No. 4, 1996, pp. 541–563.
- [7] Hill, K., Alfriend, K.T., Sabol, C., “Covariance-based Uncorrelated Track Association,” AIAA 2008-7211, 2008 AIAA/AAS Astrodynamics Specialist Conference, Honolulu, HI, August 2008.
- [8] Sabol, C., Sukut, T., Hill, K., Alfriend, K. T., Wright, B., and Schumacher, P., “Linearized Orbit Covariance Generation and Propagation Analysis via Simple Monte Carlo Simulations”, AFRL-RD-PS, TP-2010-1009.
- [9] Mahalanobis, P.C., “On the Generalized Distance in Statistics,” Proceedings of the National Institute of Sciences of India, Vol. 2, pp. 49–55.
- [10] Seago, J. H. and Vallado, D.A., “Goodness of Fit Test for Orbit Determination,” AAS 10-149, 2010 AAS/AIAA Space Flight Mechanics Conference, San Diego, CA, February 2010.
- [11] Vallado, D. A. and Seago, J.H., “Covariance Realism,” AAS 09-304, 2009 AAS/AIAA Astrodynamics Specialist Conference, Pittsburgh, PA, August 2009.

- [12] Henderson L.S., Coppola, V., “Statistical Tests for Gaussian Mean and Covariance in Orbit Propagation”, AAS 13-204, 23rd AAS/AIAA Space Flight Mechanics Meeting, Kauai, HI, February 2013.
- [13] Julier, S.J., Uhlmann, J. K., and Durrant-Whyte, “A New Method for the Nonlinear Transformation of Means and Covariances in Filters and Estimators,” Technical Note in IEEE Transactions on Automatic Control, Vol. 45, No. 3, March 2000, pp. 477–482.
- [14] Julier, S.J., and Uhlmann, J. K., “A new extension of the Kalman Filter to Non-linear Systems,” AeroSense: The 11<sup>th</sup> International Symposium on Aerospace/Defense Sensing, Simulation and Controls, Orlando, FL, 1997.
- [15] Julier, S.J., and Uhlmann, J. K., “The scaled unscented transformation,” 2002 American Control Conference, Anchorage, AK, pp. 4555–4559.
- [16] Vallado, D.A., Alfano, S., “Curvilinear coordinate transformations for relative motion,” Celestial Mechanics and Dynamical Astronomy, Vol. 118, No. 3 (2014), pp. 253–271.
- [17] <http://www.agi.com/products/stk/modules/default.aspx/id/stk-free>.
- [18] Vallado, D.A., Hujsak, R., Johnson, T., Seago, J., Woodburn, J., “Orbit Determination Using ODTK Version 6”, European Space Astronomy Centre, Madrid, Spain, May 2010.
- [19] DeMars, K. J., and Jah, M.K., "Probabilistic Initial Orbit Determination Using Gaussian Mixture Models", Journal of Guidance, Control, and Dynamics, Vol. 36, No. 5 (2013), pp. 1324-1335.
- [20] DeMars, K. J., Jah, M.K., Giza, D., and Kelecy, T. "Orbit Determination Performance Improvements for High Area-To-Mass Ratio Space Object Tracking Using an Adaptive Gaussian Mixtures Estimation Algorithm," 21<sup>st</sup> International Symposium on Space Flight Dynamics, Toulouse, France, September 2009.